Spectroscopic study of transparency current in mid-infrared quantum cascade lasers

Dmitry G. Revin,[1,*] Randa S. Hassan,[1,4] Andrey B. Krysa,[2] Yongrui Wang,[3] Alexey Belyanin,[3] Kenneth Kennedy,[2] Chris N. Atkins,[1] and John W. Cockburn[1]

[1]*Department of Physics and Astronomy, The University of Sheffield, Sheffield S3 7RH, UK*
[2]*Department of Electronic and Electrical Engineering, EPSRC National Centre for III-V Technologies, The University of Sheffield, Sheffield S1 3JD, UK*
[3]*Department of Physics and Astronomy, Texas A&M University, College Station, Texas 77843 USA*
[4]*National Institute of Laser Enhanced Sciences (NILES), Cairo University, Cairo, Egypt*
[*]*d.revin@sheffield.ac.uk*

Abstract: We report measurements which give direct insight into the origins of the transparency current for λ ~5 μm $In_{0.6}Ga_{0.4}As/In_{0.42}Al_{0.58}As$ quantum cascade lasers in the temperature range of 80-280 K. The transparency current values have been found from broadband transmission measurements through the laser waveguides under sub-threshold operating conditions. Two active region designs were compared. The active region of the first laser is based on double-LO-phonon relaxation approach, while the second device has only one lower level, without specially designed resonant LO-phonon assisted depopulation. It is shown that transparency current contributes more than 70% to the magnitude of threshold current at high temperatures for both designs.

OCIS codes: (140.5965) Semiconductor lasers, quantum cascade; (300.6340) Spectroscopy, infrared.

References and links

1. J. Faist, F. Capasso, D. L. Sivco, C. Sirtori, A. L. Hutchinson, and A. Y. Cho, "Quantum cascade laser," Science **264**(5158), 553–556 (1994).
2. A. Lyakh, R. Maulini, A. Tsekoun, R. Go, and C.K.N. Patel, "Tapered 4.7 μm quantum cascade lasers with highly strained active region composition delivering over 4.5 Watts of continuous wave optical power," Opt. Express **20**(4), 4382–4388 (2012).
3. Y. Bai, N. Bandyopadhyay, S. Tsao, S. Slivken, and M. Razeghi, "Room temperature quantum cascade lasers with 27% wall plug efficiency," Appl. Phys. Lett. **98**(18), 181102 (2011).
4. R. P. Green, A. B. Krysa, J. S. Roberts, D. G. Revin, L. R. Wilson, E. A. Zibik, W. H. Ng, and J. W. Cockburn, "Room temperature operation of InGaAs/AlInAs quantum cascade lasers grown by metalorganic vapor phase epitaxy," Appl. Phys. Lett. **83**(10), 1921–1922 (2003).
5. D. G. Revin, L. R. Wilson, J. W. Cockburn, A. B. Krysa, J. S. Roberts, and R. J. Airey, "Intersubband spectroscopy of quantum cascade lasers under operating conditions," Appl. Phys. Lett. **88**(13), 131105 (2006).
6. H. Willenberg, G. H. Döhler, and J. Faist, "Intersubband gain in a Bloch oscillator and quantum cascade laser," Phys. Rev. B **67**(8), 085315 (2003).
7. R. Terazzi, T. Gresch, M. Giovannini, N. Hoyler, N. Sekine, and J. Faist, "Bloch gain in quantum cascade lasers," Nat. Phys. **3**(5), 329–333 (2007).
8. D. G. Revin, M. R. Soulby, J. W. Cockburn, Q. Yang, C. Manz, and J. Wagner, "Dispersive gain and loss in midinfrared quantum cascade laser," Appl. Phys. Lett. **92**(8), 081110 (2008).
9. A. Wittmann, T. Gresch, E. Gini, L. Hvozdara, N. Hoyler, M. Giovannini, and J. Faist, "High-performance bound-to-continuum quantum cascade lasers for broad-gain applications," IEEE J. Quantum Electron. **44**(1), 36–40 (2008).
10. R. Maulini, A. Lyakh, A. Tsekoun, R. Go, C. Pflügl, L. Diehl, F. Capasso, and C.K.N. Patel, "High power thermoelectrically cooled and uncooled quantum cascade lasers with optimized reflectivity facet coating," Appl. Phys. Lett. **95**(15), 151112 (2009).
11. J. S. Yu, S. Slivken, A. J. Evans, and M. Razeghi, "High-performance continuous wave operation of λ ~ 4.6 μm quantum cascade lasers above room temperature," IEEE J. Quantum Electron. **44**(8), 747–754 (2008).

#169082 - $15.00 USD Received 23 May 2012; revised 23 Jul 2012; accepted 24 Jul 2012; published 2 Aug 2012

12. E. Benveniste, S. Laurent, A. Vasanelli, C. Manquest, C. Sirtori, F. Teulon, M. Carras, and X. Marcadet, "Measurement of gain and losses of a midinfared quantum cascade lasers by wavelength chirping spectroscopy," Appl. Phys. Lett. **94**(8), 081110 (2009).
13. Y. Dikmelik, J. B. Khurgin, M. D. Escarra, P. Q. Liu, and C. F. Gmachl, "Temperature dependence of the transparency current density in mid-infrared quantum cascade lasers," in *Conference on Lasers and Electro-Optics* 2011, Technical Digest (CD) (Optical Society of America, Washington, DC, 2011), paper CTuC2.
14. C. Sirtori, H. Page, C. Becker, and V. Ortiz, "GaAs-AlGaAs quantum cascade lasers: Physics, Technology, and Prospects," IEEE J. Quantum Electron. **38**(6), 547–558 (2002).

Introduction

Recently, mid-infrared quantum cascade lasers (QCLs) [1] have achieved a remarkable level of performance, emitting several Watts of continuous optical power at room temperature [2, 3]. This performance has become possible due to careful optimization of the laser parameters and continuing advances in device processing and packaging. However, in most cases high threshold currents are still a problem and the origin and the value of transparency current are increasingly thought to be an important factors that have not yet been studied experimentally in great detail. The transparency current corresponds to the current through the laser at the point when the increasing gain at the laser transition is equal to the losses at this transition. In a simplified theoretical analysis of mid-infrared QCLs it is still widely assumed that transparency current is virtually zero, in contrast to the case for interband lasers. Any small current through a QCL is supposed to create intersubband population inversion and result in gain. However, such a suggestion is only valid if there are no electrons on the lower laser level and the current flows only by injection of the carriers into the upper laser level. The first requirement can be easily fulfilled for the optimum active region designs, albeit only for very low temperatures. The second is more problematic, since there can be phonon-assisted leakage transport of electrons from the injector directly to the lower laser levels or escape of electrons to the continuum through the injector upper minibands, suppressing the onset of population inversion.

In the present paper we report detailed investigations of transparency current in mid-infrared QCLs at various temperatures, by means of broadband transmission spectroscopy of devices under sub-threshold operating conditions. We show that at 280 K the transparency current constitutes more than 70% of the threshold current value for typical QCL designs.

Laser designs and experimental setup

Two laser designs have been studied for comparison, based on strain-compensated $In_{0.6}Ga_{0.4}As/Al_{0.58}In_{0.42}As$ QCL wafers with laser cores comprising 35 periods of the active and injector regions. The first design (S1) is based on a double-LO-phonon relaxation approach with the layer sequence (thicknesses, in nm), starting with the injector barrier: **4**/1.3/**1.3**/5.1/**1.3**/4.5/**1.4**/4/**2.3**/3.1/**1.8**/2.8/**1.9**/2.5/**2**/2.4/**2.2**/2.3/**2.8**/2.2, where $Al_{0.58}In_{0.42}As$ barriers are in the bold font and underlined layers are doped with Si to $n = 1 \times 10^{17}$ cm^{-3}. It is usually assumed that two levels positioned below the lower laser level and separated by the energy close to the LO phonon energy should provide efficient depletion of the lower laser level, therefore helping to achieve population inversion. For the second wafer (S2) the exit barrier (2.3 nm thick as in the first design) is moved to be closer to the injection barrier: **4**/1.3/**1.3**/5.2/**2.4**/4.5/**1.7**/4/**1.7**/3.1/**1.8**/2.8/**1.9**/2.5/**2**/2.4/**2.2**/2.3/**2.8**/2.2, creating just one wide quantum well (5.2 nm thick) in the active region without specially designed resonant LO-phonon assisted depopulation.

The wafers were grown on highly doped ($n \sim 10^{18}$ cm^{-3}) InP substrates by metal organic vapour phase epitaxy [4]. The laser core regions are grown between 0.3 μm thick $In_{0.53}Ga_{0.47}As$ spacer layers ($n = 5 \times 10^{16}$ cm^{-3}) and 2.5 μm thick low doped ($n = 5 \times 10^{16}$ cm^{-3}) InP waveguide layers. The wafers were capped with 0.8 μm highly doped ($n = 7 \times 10^{18}$ cm^{-3}) InP top claddings.

#169082 - $15.00 USD Received 23 May 2012; revised 23 Jul 2012; accepted 24 Jul 2012; published 2 Aug 2012

The wafers were processed by dry etching into 20 μm wide ridge lasers. Thermally evaporated, annealed Ti/Au top and InGa/Au bottom contacts were used. 5 μm thick electroplated gold was deposited on top of the ridges to improve heat dissipation from the devices. The laser chips were indium-soldered epilayer-up on copper submounts. The mounted lasers were then fixed on a cold finger of a continuous flow helium cryostat. The broadband mid-infrared emission from a FTIR spectrometer was focused on to the front facet of the laser ridge and the light transmitted through the laser waveguide was detected by a cooled mercury-cadmium telluride detector. The experimental setup is very similar to that described in [5]. Due to the selection rules applicable to the intersubband electron transitions in quantum wells, TM (parallel to the growth direction) polarized light was used for the transmission measurements. To eliminate waveguide absorption effects (assumed to be independent of polarization), the TM transmission spectra were divided by the spectra taken at the TE polarization. The spectral resolution is about 5 meV. DC bias below the laser thresholds was applied to the lasers under investigation.

Transmission measurements

The transmission spectra in the energy range around the laser transitions were studied at temperatures of 80, 120, 160, 200, 240 and 280 K and for various current values below the threshold for 2 mm long laser S1 and 2.5 mm long laser S2. The spectra taken at 80 and 240 K are shown in Fig. 1. The dips correspond to the absorption or the losses at particular energy, while the peaks represent the amplification of the incident light or, in other words, the presence of gain. At 80 K no absorption is observed for S1 at the laser energy for any current. This is a direct demonstration of a double-phonon design working at low temperatures as theoretically predicted when the lower laser level stays empty due to efficient LO-phonon assisted electron relaxation. At elevated applied bias the amplification peak gradually increases at the energy of the laser transition (230 meV).

For laser S2 at low current, even at temperatures as low as 80 K (Fig. 1(b)), there is strong absorption at the laser energy, indicating that in this case the lower laser level is populated with the electrons from the doped layers of the injector. Such a strong absorption at the laser transition (high concentration of the electrons on the lower laser level) exists for laser S2 at low current for all temperatures. The intensity of the transmitted light increases with bias and, similar to S1, at certain bias the gain starts building up at the energy of the laser transition (253 meV for laser S2).

For laser S1 the absorption at the energy of the laser transition (signalling the presence of electrons on the lower laser level) is however, observed starting from the temperatures higher than ~120 K. This indicates that even for this phonon-assisted-depopulation laser design hot electrons from the injector occupy the lower laser level at these temperatures (see Fig. 1(c)).

At high temperatures the transmission experiments reveal very distinct features of the amplification and absorption peaks. For some values of current the spectra near the laser transition have a dispersive shape, when the absorption and amplification are observed at the same time but at slightly different energies (Fig. 1(c) and 1(d)). Similar behavior has been previously observed in mid-infrared QCLs and studied both theoretically [6] and experimentally [7, 8]. In these works it was suggested that for the cases when the populations of the electrons on the upper and lower laser levels are comparable, the existence of the scattering processes, particularly at higher temperatures, leads to the increased contribution of the second order gain which results in a dispersive shape.

The gain value can be scaled as the product of the gain cross-section g and the population difference, so the transmitted light intensity is proportional to $\exp(g(n_2 - n_1)L)$, where $n_{2,1}$ are the electron concentrations (dependent on current) on the upper and lower laser levels respectively, and L is the laser length. The logarithms of the light intensities of the absorption dips and amplification peaks normalized to the laser cavity lengths are shown in Fig. 2 for

#169082 - $15.00 USD Received 23 May 2012; revised 23 Jul 2012; accepted 24 Jul 2012; published 2 Aug 2012

both lasers. At the bias well below the laser alignment, there are more electrons on the lower laser level compared to the upper level ($n_1 >> n_2$) and as the observed dependence of the absorption intensities on increasing current (see Fig. 2) is almost exponential it can be assumed that n_1 reduces linearly with increasing current.

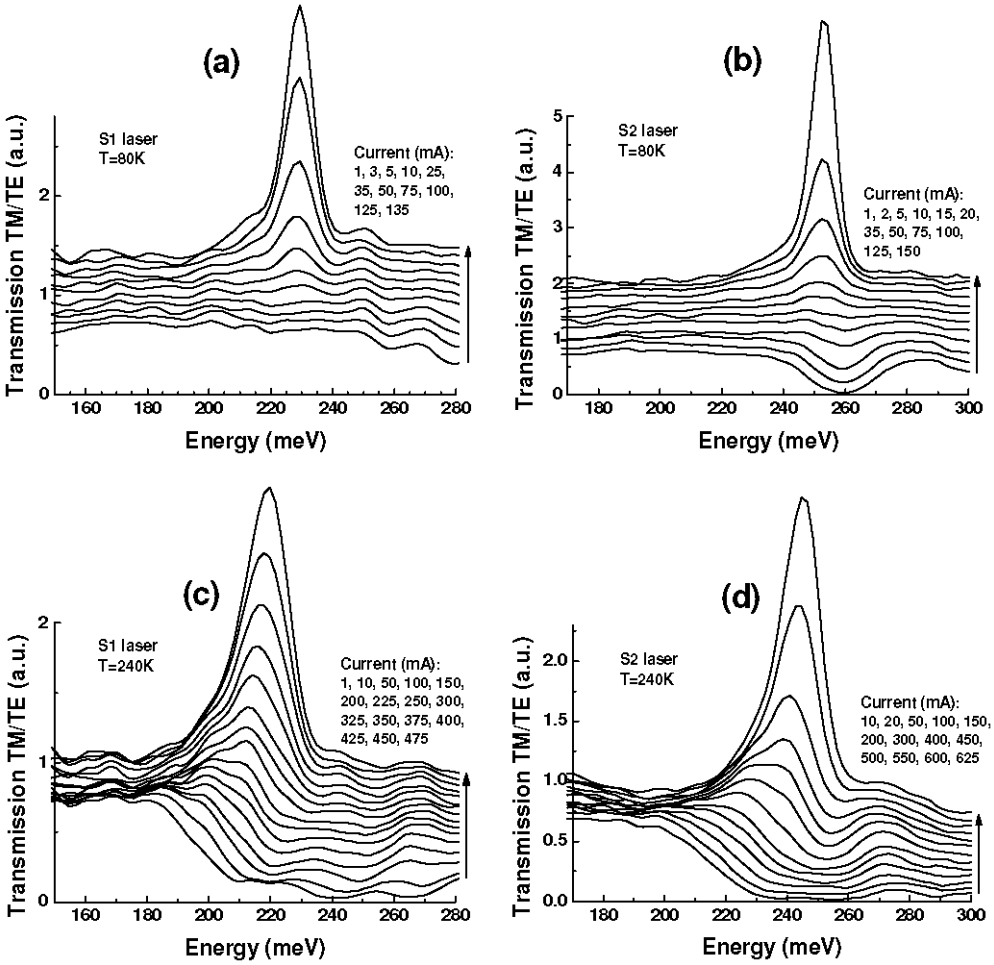

Fig. 1. Experimental transmission spectra (taken for TM polarization and normalized for the spectra taken for TE polarization) for lasers S1 and S2 measured at 80 and 240 K for various current values below the laser thresholds. The spectra are vertically shifted for clarity where the spectra presented as the lowest were measured for the smallest current values. The absorption peaks observed at the energies higher than the laser transitions correspond to other intersubband transitions in the QCL active regions (see [5], for example).

The intensities of the absorption peaks for laser S2, extrapolated to zero current, converge to nearly the same value (marked by the black square in Fig. 2(b)) for all temperatures (80 - 280 K). The band structure simulations show that at zero bias the lower laser level in device S2 is the overall ground state of the laser period consisting of the active region and doped injector; therefore, almost all electrons from the injector are residing on the lower laser level. For laser S1 the absorption appears only at temperatures above 120 K; (see Fig. 2(a)) when thermally excited electrons start to populate the lower laser level. The electron population on this level gradually increases with the temperature but it is still lower than for device S2, even at 280 K. n_1 reduces with increasing bias for both lasers. However, at the elevated temperatures the rate of this reduction of the electron concentration with increasing current

#169082 - $15.00 USD Received 23 May 2012; revised 23 Jul 2012; accepted 24 Jul 2012; published 2 Aug 2012

decreases because thermal backfilling of the electrons from the injector increases. These measurements directly show that the thermal back-filling process is less pronounced for S1 compared to S2, consistent with expectations.

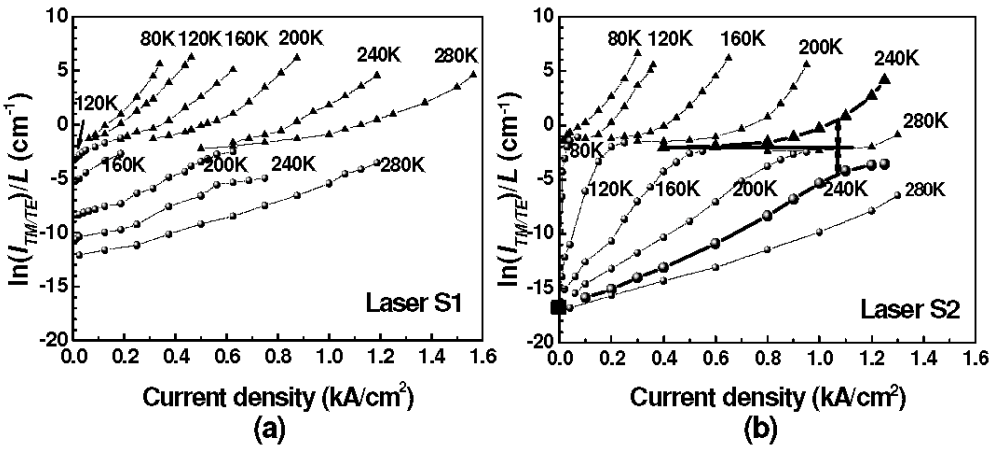

Fig. 2. The logarithm ($\ln(I_{TM/TE})/L$) of the intensities of the amplification peaks (upper curves, ▲) and the absorption dips (lower curves, ●), extracted from the TM/TE transmission spectra and normalized by the cavity length *L*, versus the current density for QCLs S1 (a) and S2 (b). The horizontal and vertical thick black lines show the example on how the transparency current for laser S2 was estimated from the data at 240 K.

The dependence of the intensity of the amplification peaks on current density can be fitted by the exponential curve only in the current range close to the threshold (Fig. 2). For the bias close to the laser alignment the injection of the electrons to the upper laser level becomes very efficient and we can assume that $n_2 >> n_1$. Then our measurements directly demonstrate that the gain formation does not start straightaway at very small current values but appears after some given value of the current and this "onset" current increases with temperature.

One of the formal descriptions of such transparency current density (J_{tr}) in experiments with QCLs is the introduction of additional intersubband resonant losses $\alpha_{res} = GJ_{tr}$, originating from the electrons residing on the lower laser level [9–11] so the equation for the threshold current density is therefore modified as follows: $J_{th} = (\alpha_w + \alpha_m + \alpha_{res})/G = (\alpha_w + \alpha_m)/G + J_{tr}$, where α_w is the waveguide losses, α_m is the mirror losses and *G* is the modal gain coefficient.

However, by using the transmission spectra data presented here it is possible to directly determine the transparency current for the operating devices. The transparency current is assumed to correspond to the bias condition when the gain is the same as the losses at the energies near to the laser transition. The method of extracting the transparency current values from our measurements can be explained by taking, as an example, the dependence for the transmission light intensities for laser S2 at 240 K. (We note that when the transmission spectra has the dispersive shape both amplification and absorption are observed even for $n_2 = n_1$.) The thick black horizontal line in Fig. 2(b) represents the intensity of the transmitted light observed at low bias when there is no gain in the laser. Then the current value is found which corresponds to the position where the distances to the amplification and absorption curves (the vertical thick black lines with the arrows) are equal. This current value is the transparency current as at this point the gain is equal to the losses. J_{tr} found from the transmission experiments and J_{th} measured in the pulsed regime with 50 ns pulses at 5 kHz repetition rate are shown in Fig. 3 for both lasers. The small difference in the length of the ridges of the studied lasers should be noted (laser S1 is shorter and therefore has higher mirror

#169082 - $15.00 USD Received 23 May 2012; revised 23 Jul 2012; accepted 24 Jul 2012; published 2 Aug 2012

losses) which results in J_{th} being slightly less for laser S2 at 80 and 120 K than for laser S1. The transparency current as percentage value of the threshold current is higher for laser S2 confirming the advantage of the double-LO-phonon designs. However, the transparency current increases rapidly with temperature for both lasers and contributes more than 70% to the threshold current at high temperatures even for the laser with the double-LO-phonon design. The measured contribution of the transparency current is similar to that reported in other publications [11–13], where it was estimated that the transparency current makes up more than half of the threshold current. Another possible explanation [14] also supported by our theoretical simulations is that at elevated temperatures and for the voltage values below the voltage at threshold the current flows in part due to scattering from the bottom of the injector directly to the lower laser level.

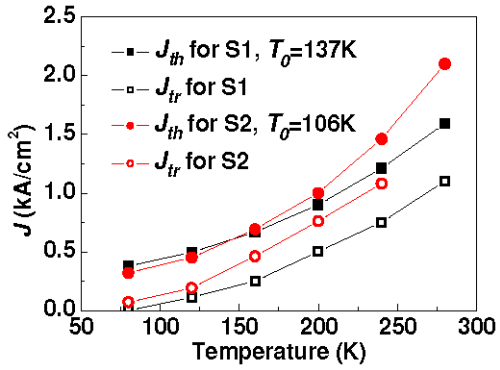

Fig. 3. Threshold J_{th} and transparency J_{tr} current densities for QCLs S1 and S2 in the temperature range of 80-280 K. T_0 values have been extracted from the fitting J_{th} ~exp(T/T_0).

Conclusion

The detailed spectroscopic investigation of the origin and the values of the transparency current has been carried out for two InGaAs/InAlAs quantum cascade lasers with different designs. Rapid increase of the transparency current with temperature was observed not only for the laser with much suppressed electron depopulation from the lower laser level but also for the laser with nearly optimized active region design based on the double-LO-phonon assisted depopulation of the electrons from the lower laser level. It has been demonstrated that the transparency current contributes significantly (more than 70% at 280 K) to the threshold current for both lasers and originates partly due to temperature defined processes such as thermal backfilling and scattering assisted leakage from the injector directly to the lower laser levels.

Acknowledgments

This work is partly supported by the Engineering and Physical Sciences Research Council (EPSRC) UK under Grant No. EP/H050655/1. Y.W. and A.B. also acknowledge partial support from NSF grants EEC-0540832 and ECCS-0925446, and from the NHARP Project No. 003658-0010-2009. R. H. thanks the Egyptian Ministry of Higher Education for the award of a Ph.D studentship.

#169082 - $15.00 USD Received 23 May 2012; revised 23 Jul 2012; accepted 24 Jul 2012; published 2 Aug 2012